

# Symmetrisation in the Interaction of Chloro[2-(dimethylaminomethyl)phenyl-C<sup>1</sup>]mercury(II) with Thiosemicarbazone Derivatives of Pyridine-2-carboxamide and Pyrazin-2-carboxamide

Ulrich Abram,<sup>[b]</sup> Alfonso Castiñeiras,<sup>\*[a]</sup> Isabel García-Santos,<sup>[a]</sup> and Raul Rodríguez-Riobó<sup>[a]</sup>

**Keywords:** Mercury complexes / Symmetrisation / Thiosemicarbazones / Crystal structures / Weak hydrogen bonds / C–H... $\pi$  interactions

Pyridine- and pyrazine-2-carboxamide thiosemicarbazones (HAm4DH and HAm4DM) or their *N*<sup>4</sup>,*N*<sup>4</sup>-dimethyl derivatives (HAm4DM and HAm4DM) react with chloro[2-(dimethylaminomethyl)phenyl-C<sup>1</sup>]mercury(II), [Hg(damp)Cl], to give the tetrahedral [Hg(TSC)<sub>2</sub>] complexes [TSC = Am4DH (1), Am4DM (2), Ampz4DH (3) or Ampz4DM (4)]. Spectroscopic studies and a X-ray structural analysis show that the potentially tridentate thiosemicarbazones adopt S,N coordination modes, with each deprotonated thiosemicarbazone binding to the Hg<sup>II</sup> centre through the azomethine ni-

trogen and the thiolate sulfur atoms, whereas the heterocyclic nitrogen atoms are free of coordination. Intra- and intermolecular hydrogen bonding in all complexes and specific C–H... $\pi$  interactions with the chelate or pyridyl rings of the complexes 1 and 2 were found in the crystal structures. Furthermore, [Hg(damp)Cl] undergoes symmetrisation to give the symmetric unit [Hg(Hdamp)<sub>2</sub>]<sup>2+</sup> in which the Hdamp is protonated at the nitrogen.

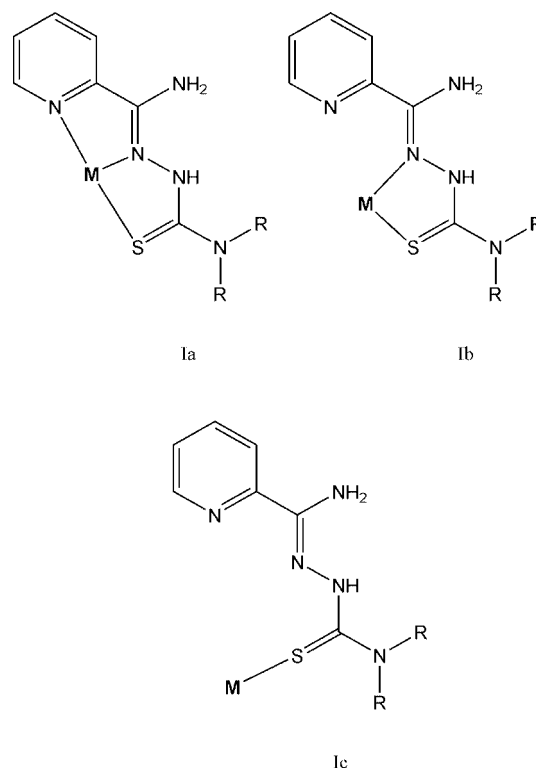
(© Wiley-VCH Verlag GmbH & Co. KGaA, 69451 Weinheim, Germany, 2006)

## Introduction

Thiosemicarbazones have been extensively studied due to their pharmacological properties and their coordinative behaviour towards transition-metal ions.<sup>[1]</sup> However, very few mercury(II) complexes with thiosemicarbazones are known.

The reaction of potentially tridentate thiosemicarbazones, such as 2-acetylpyridine thiosemicarbazone or pyridine-2-carboxamide thiosemicarbazone, with Hg<sup>II</sup> salts gives rise to five-coordinate compounds [Hg(HL)X<sub>2</sub>] (X = Cl, Br or I) in which coordination to the metal centre occurs through the pyridine and azomethine nitrogen atoms and the thiocarbonyl sulfur atom (Scheme 1, a).<sup>[2–6]</sup> Furthermore, compounds such as 2-acetylpyridine *N*-oxide *N*<sup>4</sup>,*N*<sup>4</sup>-dimethylthiosemicarbazone can act as N,S-bidentate ligands for mercury halides in which the metal atom has a coordination number four with the same formula [Hg(HL)X<sub>2</sub>] for the complexes (Scheme 1, b).<sup>[7]</sup> These thiosemicarbazones can also form dimeric or polymeric complexes in which the sulfur or the halogen acts as a bridge between metal centres and, in some cases, they also behave as S-monodentate ligands (Scheme 1, c) to form complexes of

the formula [Hg(HL)<sub>2</sub>X<sub>2</sub>], where the mercury atom has a tetrahedral coordination geometry.<sup>[5,6,8,9]</sup>



Scheme 1.

[a] Departamento de Química Inorgánica, Facultad de Farmacia, Universidad de Santiago de Compostela, 15782 Santiago de Compostela, Spain  
Fax: +34-981547-163  
E-mail: qiac01@usc.es

[b] Freie Universität Berlin, Chemisches Institut, Fabeckstr. 34–36, 14195 Berlin, Germany

Pyridine-2-carboxamide and pyrazine-2-carboxamide thiosemicarbazone derivatives (Figure 1) are almost always N,N,S-tridentate ligands<sup>[2–6]</sup> but are sometimes unidentate ligands that coordinate through the sulfur atom.<sup>[6]</sup> Only in two rhenium complexes does the 2-cyanopyridine thiosemicarbazone act as an N,N-bidentate ligand through the pyridine and azomethine nitrogen atoms (Scheme 2, a)<sup>[10]</sup> or through the amide and imine nitrogen atoms (Scheme 2, b).<sup>[11]</sup>

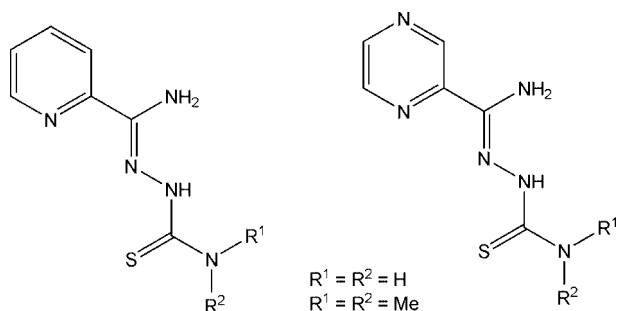
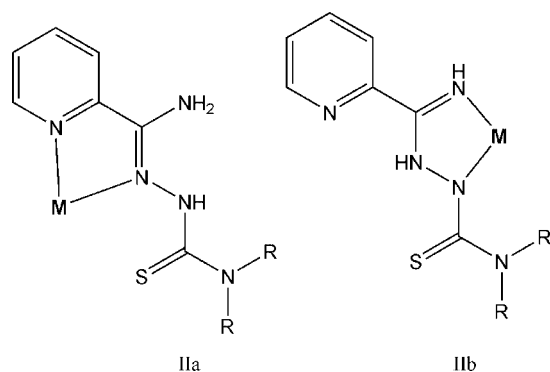


Figure 1. Pyridine-2-carboxamide and pyrazine-2-carboxamide thiosemicarbazone derivatives (left and right, respectively).



Scheme 2.

The coordination chemistry of organomercury(II) is not as extensive as that of mercury(II) salts such as halides or pseudohalides, probably because organomercury(II) derivatives have a lower tendency to increase their coordination by interaction with donor molecules. Organomercury(II) substrates,  $\text{RHgX}$ , are known to undergo symmetrisation to form symmetric diorganomercury  $\text{HgR}_2$  and  $\text{Hg}^{\text{II}}$  complexes.<sup>[12–15]</sup> Bidentate thiosemicarbazones react with organomercury(II) ( $\text{RHgX}$ ) to form three-coordinate complexes  $[\text{HgR}(\text{TSC})]$  ( $\text{R} = \text{Ph}$  or  $\text{Me}$ ,  $\text{TSC} = \text{thiosemicarbazone}$ ).<sup>[16–18]</sup>

When “TSC” is benzaldehyde or 4-methoxybenzaldehyde, the  $^{199}\text{Hg}$  NMR spectrum shows two signals, one corresponding to the formation of the aforementioned complex and another corresponding to the formation of  $\text{HgPh}_2$ , indicating that a symmetrisation reaction has occurred. However, when the “TSC” is cyclopentanone, cyclohexanone, 2-hydroxybenzaldehyde, *N*-phenyl pyrrole-2-carbaldehyde, *N*-phenyl thiophene-2-carbaldehyde, or furan-2-carbaldehyde thiosemicarbazone, the  $^{199}\text{Hg}$  spectra show only one signal, indicating the presence of a single type of chemical en-

vironment around the mercury(II) atom. The reaction between acetophenone thiosemicarbazone (Hatsc) and  $\text{PhHgCl}$  gives compounds of formula  $[\text{HgCl}_2(\text{Hatsc})_2]$ , where the proposed structure is a four-coordinate complex in which the “Hatsc” is bonded to the metal through the thiocarbonyl sulfur atom, and  $\text{Ph}_2\text{Hg}$  as the products of the symmetrisation reaction.<sup>[19]</sup>

In this paper we report the first examples of the reactions between pyridine-2-carboxamide or pyrazine-2-carboxamide thiosemicarbazone (HAm4DH and HAm4DM) and their  $N^4,N^4$ -dimethyl derivatives (HAm4DM and HAm4DM), which are usually N,N,S-tridentate ligands, with chloro[2-(dimethylaminomethyl)phenyl- $\text{C}^1$ ]mercury(II) (Figure 2). These reactions give complexes  $[\text{Hg}(\text{Am4DH})_2]$  (**1**),  $[\text{Hg}(\text{Am4DM})_2]$  (**2**),  $[\text{Hg}(\text{Ampz4DH})_2]$  (**3**) and  $[\text{Hg}(\text{Ampz4DM})_2]$  (**4**), which contain two deprotonated ligands in a bidentate mode chelating to the  $\text{Hg}^{\text{II}}$  through the azomethine nitrogen and thiolate sulfur atoms, a very unusual coordination mode for these potentially tridentate ligands. Furthermore, the  $^{199}\text{Hg}$  NMR spectroscopic data suggest a symmetrisation phenomenon, which is also supported by  $^1\text{H}$  NMR and IR data. In contrast to this behaviour, it was recently reported that thiosemicarbazone complexes of gold(III) are formed in reactions of  $[\text{Au}(\text{damp}^-\text{C},\text{N})\text{Cl}_2]$  with pyridine-2-carboxamide thiosemicarbazones, where the organometallic damp $^-$  ligand is protonated during the reactions and the  $\text{Au}-\text{N}$  bond is cleaved.<sup>[20]</sup>

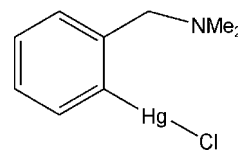


Figure 2. Chloro[2-(dimethylaminomethyl)phenyl- $\text{C}^1$ ]mercury(II).

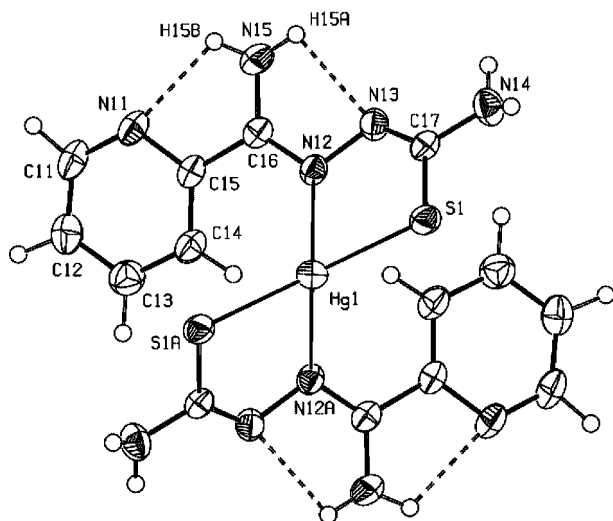
## Results and Discussion

The reaction of chloro[2-(dimethylaminomethyl)phenyl- $\text{C}^1$ ]mercury(II),  $[\text{Hg}(\text{damp})\text{Cl}]$ , with pyridine-2-carboxamide or pyrazine-2-carboxamide thiosemicarbazone (HAm4DH and HAm4DM) and their  $N^4,N^4$ -dimethyl derivatives (HAm4DM and HAm4DM) give solids of formula  $[\text{Hg}(\text{TSC})_2]$  ( $\text{TSC} = \text{deprotonated thiosemicarbazone}$ ). The products are consistent with the elemental analysis data and are colourless or yellow and quite soluble in common organic solvents.

The  $\text{FAB}^+$  spectra of all complexes show peaks corresponding to  $\{\text{H}_2\text{L}\}^+$ , but only the  $N^4,N^4$ -dimethyl-substituted complexes show fragments that contain mercury. The spectra of **2** and **4** show peaks at  $m/z = 646$  and  $m/z = 648$ , which can be assigned to a molecular ion of composition  $\{\text{HgHL}_2\}^+$ . Peaks at  $m/z = 423$  can be assigned to the complex with a loss of a ligand,  $\{\text{HgL}\}^+$ . In the mass spectra of **1** and **3** only the signals due to the protonated ligand can be seen (at  $m/z$  196 and 197, respectively).

## X-ray Crystal Structures

In the molecular structures of the complexes the geometry is essentially similar and contains four coordinate neutral  $\text{Hg}(\text{TSC})_2$  molecules. However, in the compounds **1**, **3** and **4** the mercury atom lies on a twofold axis and the asymmetric unit consists of half a molecule of complex and, as a consequence, a tetrahedral complex is formed with two chelating anionic ligands around the central metal (Figure 3). Complex **2** crystallises in the orthorhombic space group  $Pna2_1$  and the Hg metal ion is tetrahedrally coordinated with two symmetrically independent thiosemicarbazone ligands as monoanionic bidentate N,S-chelators (Figure 4). Selected bond lengths and angles are listed in Table 1 and Table 2, respectively.



second thiosemicarbazone (**2**) [av. 0.2874(2) Å] (Figure 5). These coordination planes form angles in the range 5.5(1)–12.0(2)° (**1**, **3** and **4**) and 16.2(4)–36.2(2)° (**2**) with the mean plane of the thiosemicarbazone moiety.

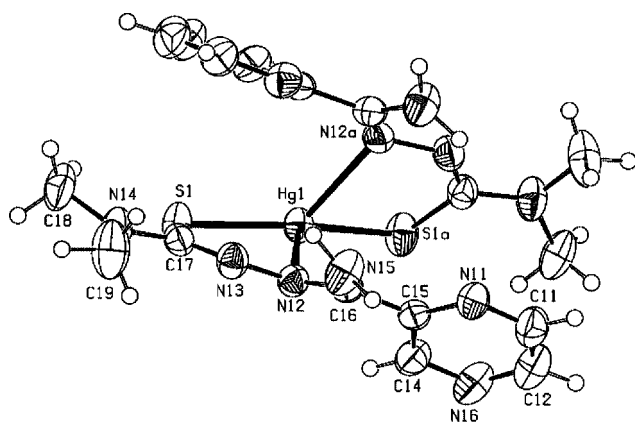


Figure 5. Perspective drawing of **4** oriented as a distorted trigonal pyramid. Symmetry codes are as given in Table 2.

The least-squares plane data and deviations from these planes for the complexes are listed in Table 3. In all four complexes the pyridyl and pyrazinyl rings are almost planar. In complex **1** the pyridine ring and the thiosemicarbazone moiety form a dihedral angle of 44.8(1)°, and the two thiosemicarbazones bonded to the Hg<sup>II</sup> are nearly orthogonal, forming an angle of 85.3(1)°. However, in complex **2** the deviations are smaller and the angles between the pyridine and the thiosemicarbazone moieties are 25.6(8) and 29.6(7)° for the two non-symmetric ligands and the angle between the thiosemicarbazone main least-squares planes is 64.2(4)°. In complexes **3** and **4** the angles between the pyrazine ring and the thiosemicarbazone moieties are 33.3(1) and 42.7(2)°, respectively, whereas the angles between each thiosemicarbazone moiety and its symmetrical one are 46.8(1) and 45.8(2)°, respectively (Figure 6).

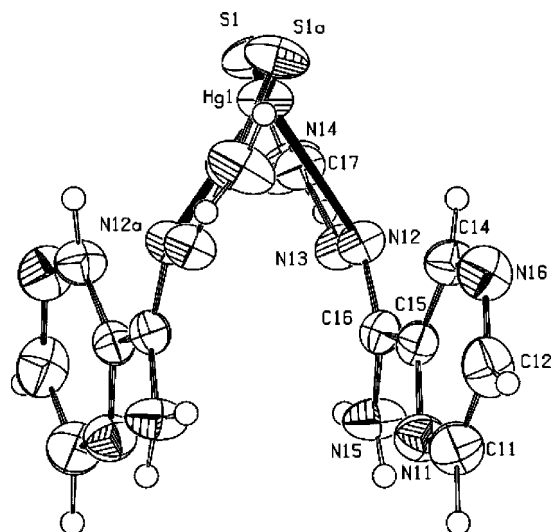


Figure 6. Parallel projection along the [010] direction showing the angle of the thiosemicarbazone moieties in the molecule of **3**. Symmetry codes are as given in Table 2.

The bond lengths in the noncoordinating pyridine and pyrazine units remain unchanged upon metal-complex formation. These units therefore appear not to participate in the complexation process. The bond lengths for the thiosemicarbazone moieties are as one would expect and the bond lengths in the five-membered chelate rings are intermediate between the usual values for single and double bonds, thus demonstrating metalloaromaticity.<sup>[22]</sup>

A number of intra- and intermolecular hydrogen bonds are formed in the crystal packing arrangement (Table 4), and it is not only the amine and imine groups that take part but also the pyridine and pyrazine nitrogen atoms of the ligands (Figure 7). The most significant intramolecular interactions occur between the amino donor groups and the imine or pyrazine nitrogen atoms of neighbouring chains, which act as acceptors. These interactions give rise to a three-dimensional supramolecular network (Figure 8).

Table 3. Best least-squares planes for complexes **1–4**.

Compound	Plane	Rms deviation [Å]	Largest deviation [Å]	Angle with previous plane [°]
<b>1</b>	S1–N12–S1 <sup>[a]</sup>	0	Hg1, 0.335(1)	
	C16–N12–N13–C17–S1–N14	0.1292	N12, 0.246(2)	9.8(1)
	N11–C11–C12–C13–C14–C15	0.0071	C14, 0.012(3)	44.8(1)
<b>2</b>	S1–N12–S2	0	Hg1, 0.215(4)	
	C16–N12–N13–C17–S1–N14	0.0080	C17, 0.02(2)	16.2(4)
	N11–C11–C12–C13–C14–C15	0.0109	C13, 0.02(2)	25.6(8)
	N21–C21–C22–C23–C24–C25	0.0139	N21, 0.02(1)	55.7(7)
	C26–N22–N23–C27–S2–N24	0.0535	N24, 0.02(1)	29.6(7)
	S2–N22–S1	0	Hg1, 0.334(4)	36.2(3)
	S1–N12–S1 <sup>[a]</sup>	0	Hg1, 0.270(1)	
<b>3</b>	C16–N12–N13–C17–S1–N14	0.0851	N12, 0.160(3)	5.5(1)
	N11–C11–C12–C13–C14–C15	0.0057	C14, 0.010(3)	33.3(1)
	S1–N12–S1 <sup>[a]</sup>	0	Hg1, 0.242(1)	
<b>4</b>	C16–N12–N13–C17–S1–N14	0.0789	N12, 0.156(4)	12.0(2)
	N11–C11–C12–N16–C14–C15	0.0126	C15, 0.021(6)	42.7(2)
	S1–N12–S1 <sup>[a]</sup>	0		

[a] Symmetry transformations used to generate equivalent atoms:  $-x, y, -z + 1/2$  (**1**, **3**);  $-x + 1, y, -z + 3/2$  (**4**).



Table 4. Hydrogen bonding interactions [ $\text{\AA}$ ,  $^\circ$ ] for complexes **1**–**4**.

	D–H...A	$d(\text{D–H})$	$d(\text{H...A})$	$d(\text{D...A})$	$\angle \text{D–H...A}$
<b>1</b> <sup>[a]</sup>	N14–H14B...N13 <sup>1</sup>	0.76	2.33	3.035(4)	154.5
	N15–H15A...N13	0.90	2.22	2.565(4)	101.8
	N15–H15B...N11	0.89	2.19	2.660(4)	112.0
<b>2</b>	N15–H15B...N11	0.86	2.35	2.69(3)	104.0
	N15–H15A...N13	0.86	2.22	2.53(2)	101.0
	N25–H25B...N21	0.86	2.33	2.67(2)	103.5
	N25–H25A...N23	0.86	2.28	2.59(2)	101.7
<b>3</b> <sup>[b]</sup>	N14–H14A...N13 <sup>1</sup>	0.91	2.24	3.142(5)	172.5
	N14–H14B...N16 <sup>2</sup>	0.83	2.24	3.060(5)	169.3
	N15–H15A...N13	0.95	2.22	2.586(4)	102.2
	N15–H15B...N11	0.88	2.24	2.660(5)	109.0
<b>4</b> <sup>[c]</sup>	N15–H15A...N13	0.97	2.27	2.579(9)	100.9
	N15–H15B...N11	0.97	2.46	2.772(9)	102.3
	N15–H15B...N16 <sup>1</sup>	0.92	2.56	3.251(10)	132.2

[a] Symmetry transformations used to generate equivalent atoms: a) 1:  $-x+1/2, y+1/2, -z+1/2$ . [b] 1:  $-x, -y+1, -z$ ; 2:  $x-1/2, -y+3/2, z-1/2$ . [c] 1:  $-x+1/2, y-1/2, -z+1/2$ .

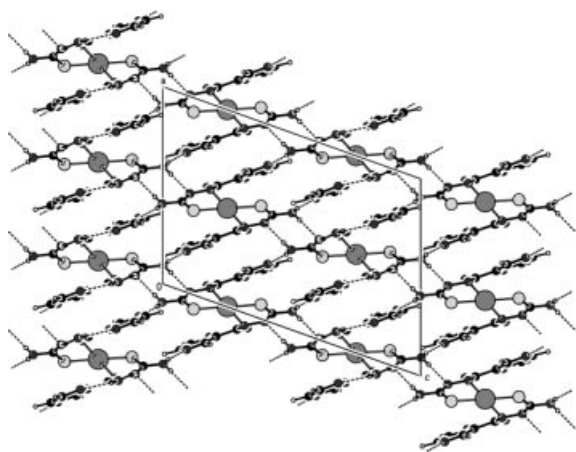


Figure 7. Drawing of the packing diagram of **3** in the  $ac$  plane showing the intermolecular hydrogen bonding and the patterns of repeating infinite array of layers along the  $[010]$  direction.

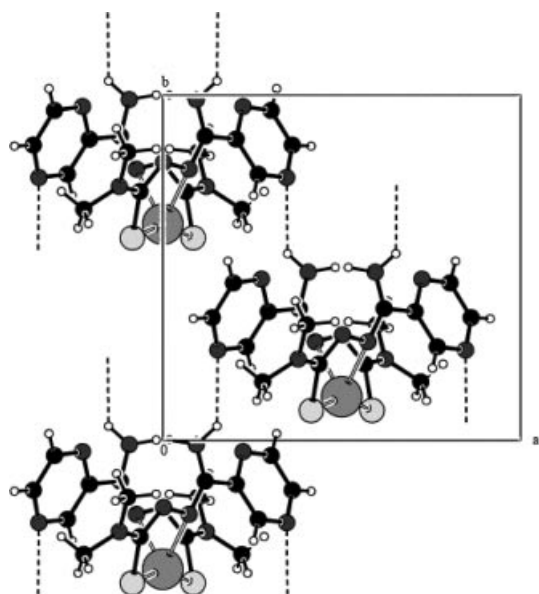


Figure 8. Partial representation of the unit cell of **4** showing the intermolecular hydrogen bonding.

Intermolecular  $\text{CH}\cdots\pi$ (chelate ring) interactions between C–H bonds of the pyridyl ligand and the metal chelate ring are observed in complex **1** (Table 5). The  $\text{H}\cdots\Omega$  (H...ring centroid) distances are in the range 2.66–2.89  $\text{\AA}$ , and the  $\alpha$  and  $\beta$  angles have values of 120° and 12.5–19.0°, respectively (Figure 9). These data are comparable with those found in crystal structures with weak  $\text{C–H}\cdots\pi$  interactions between an organic moiety and a chelate ring in transition-metal complexes ( $\alpha > 110^\circ$ ,  $\beta < 16^\circ$  and  $\text{H}\cdots\Omega < 3.0 \text{ \AA}$ ;  $\alpha$ ,  $\beta$ , and  $\Omega$  are defined in Table 5).<sup>[23]</sup> The crystal structure of complex **2** also displays a weak  $\text{C–H}\cdots\pi$  interaction between a methyl group and the pyridyl ring of neighbouring molecules.<sup>[24]</sup>

Table 5. Intermolecular  $\text{CH}\cdots\pi$  ring interaction parameters for complexes **1** and **2**.<sup>[a]</sup>

	$\text{CH}\cdots\Omega$	$\text{H}\cdots\Omega$ [ $\text{\AA}$ ]	$\alpha$ [ $^\circ$ ]	$\beta$ [ $^\circ$ ]
<b>1</b>	C11–H11...( $\text{Hg1/S1}$ ) <sup>1</sup>	2.89	120.4	12.7
	C14–H14...( $\text{Hg1/S1}$ ) <sup>2</sup>	2.66	120.9	18.9
<b>2</b>	C29–H29B...( $\text{N11/C15}$ ) <sup>3</sup>	2.97	123.6	9.5

[a]  $\Omega$  is the ring plane,  $\alpha$  the angle C–H...centroid of  $\Omega$  and  $\beta$  the angle defined by the  $\text{H}\cdots\text{centroid}$  line and the perpendicular to this plane. Symmetry transformations used to generate equivalent atoms: 1:  $-x, 1-y, -z$ ; 2:  $-x, y, 1/2-z$ ; 3:  $-x, 1-y, -1/2+z$ .

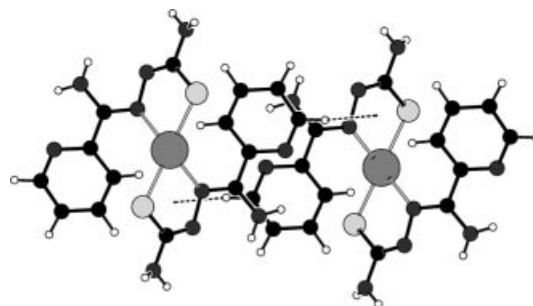


Figure 9. Perspective view of **1** showing an intermolecular  $\text{C–H}\cdots\pi$  interaction with the  $\pi$ -system of the chelate ring.

## Spectral Data

The complexes exhibit bands due to  $\nu(\text{NH})$  vibrations in the range 3500–3146  $\text{cm}^{-1}$ . The bands associated with  $\nu(\text{C=N})$  and  $\nu(\text{C=C})$  appear in the range 1609–1444  $\text{cm}^{-1}$  and are shifted to lower and higher frequencies, respectively, compared to those of the ligands. The  $\nu(\text{NH})$  band is shifted to slightly higher frequencies in the complexes with respect to the ligands, indicating the coordination of the azomethine nitrogen. The  $\nu(\text{CS})$  band appears at ca. 755  $\text{cm}^{-1}$  for the complexes with pyridine and ca. 850  $\text{cm}^{-1}$  for the pyrazine derivatives, which is in agreement with observed values for this series of compounds with the sulfur atom coordinated to the metal centre. Furthermore, coordination by the N azomethine and the S thiolate is supported by the localisation of the  $\nu(\text{Hg–N})$  modes around 405–418  $\text{cm}^{-1}$  and the  $\nu(\text{Hg–S})$  modes around 289–326  $\text{cm}^{-1}$ , respectively.

In the  $^1\text{H}$  NMR spectra of the complexes, the absence of the  $\text{N}^3\text{–H}$  signal is consistent with the thiosemicarbazone

in its deprotonated form. The pyridine proton signals appear at around 8.44–7.36 ppm and the pyrazine protons are in the range 9.67–8.48 ppm, which is normal for these aromatic protons. The N<sup>5</sup>H<sub>2</sub> proton in both **1** and **2** appear as a singlet at  $\delta = 6.60$  ppm in each case and at  $\delta = 7.06$  and 6.51 ppm for **3** and **4**, respectively. The N<sup>4</sup>H<sub>2</sub> protons appear at  $\delta = 6.03$  ppm in **1** and at 8.33, 8.22 ppm in **3**. The presence of two signals for the N<sup>4</sup>H<sub>2</sub> protons in **3** must be due to the restriction of free-rotation around the C<sup>7</sup>–N<sup>4</sup>H<sub>2</sub> bond.<sup>[19,25]</sup> The variation in the shielding between the complexes must be related to a different arrangement of the complex in DMSO solution or to a different interaction between the N<sup>4</sup>H<sub>2</sub> protons and DMSO.

The <sup>199</sup>Hg NMR spectrum of **1** shows two peaks at –577 and –806 ppm (Figure 10). The peak at  $\delta = -806$  ppm is due to our four-coordinate complex, whereas the signal at  $\delta = -577$  ppm may be due to the coordination of the nitrogen atom of the pyridine ring in DMSO solution, a situation that increases the coordination number of the Hg atom and moves the  $\delta(^{199}\text{Hg})$  signal to higher frequencies. This observation is in agreement with literature data.<sup>[25,26]</sup> Furthermore, the <sup>1</sup>H NMR spectra of the reaction between [Hg(damp)Cl] and HAm4DH in a [D<sub>6</sub>]DMSO solution shows two peaks for the protons of the pyridine ring, which is also consistent with the suggested coordination of the heterocyclic nitrogen atom in solution.

The behaviour of the complexes in solution was followed by NMR spectroscopy of the reaction between two of the thiosemicarbazones and [Hg(damp)Cl]. The <sup>199</sup>Hg NMR spectra were recorded for the reactions between [Hg(damp)Cl] and HAm4DM or HAm4DH in a MeOH/[D<sub>4</sub>]MeOH mixture in 10-mm NMR tubes. The spectra for these two reactions each show two signals (Figure 11). The first signal is observed at –650 and –655 ppm for the two reactions, respectively, and this may indicate that, in solution, the heterocyclic nitrogen atom is also coordinated to the mercury centre in the complex HgL<sub>2</sub>.<sup>[25,26]</sup> The second peak, which appears at –1162 and –1167 ppm, respectively, could correspond to the presence of [Hg(Hdamp)<sub>2</sub>]<sup>2+</sup> as a secondary product formed by symmetrisation.<sup>[13,15]</sup> These signals are shifted to higher field with respect to that of [Hg(damp)Cl],

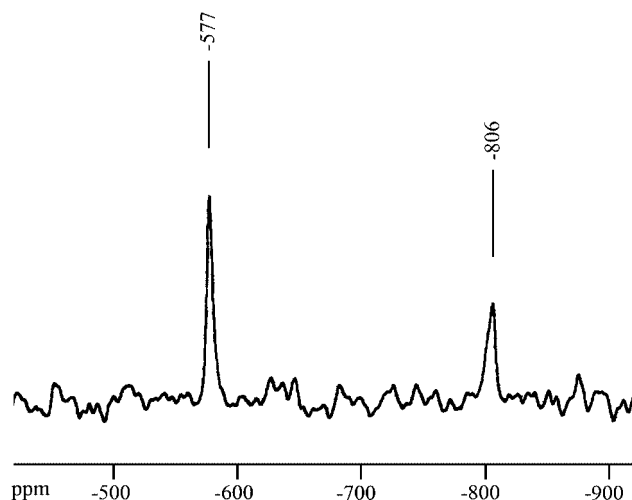


Figure 10. <sup>199</sup>Hg NMR spectrum at room temperature of a solution of complex **1** in DMSO.

which appears at  $\delta = -1109$  ppm. Symmetrisation is a well known reaction in organometallic mercury compounds<sup>[27–29]</sup> and the occurrence of such a process would be consistent with the tendency for organomercury compounds to maintain linearity in R<sub>2</sub>Hg or RHgX systems. The overall reaction can be represented as follows:

It seems likely that the most stable form of the complex in solution is Hg(TSC)<sub>2</sub><sup>(NS)</sup>, that this is the form first produced when the reaction is carried out in methanol (Scheme 3, reaction I), and that its conversion to Hg(TSC)<sub>2</sub><sup>(NS)</sup> via equilibrium II (Scheme 3) is driven by the precipitation of Hg(TSC)<sub>2</sub><sup>(NS)</sup> as crystals. When Hg(TSC)<sub>2</sub><sup>(NS)</sup> is dissolved in DMSO, equilibrium II (Scheme 3) leads rapidly to the presence of both species.

The molar conductivity values for the solutions discussed above indicate that they are 2:1 electrolytes in MeOH,<sup>[30]</sup> a finding that is consistent with the presence of the species [Hg(Hdamp)<sub>2</sub>]<sup>2+</sup> and 2 Cl<sup>–</sup>, and consequently, the formation of a zwitterionic charge distribution in this ligand is not possible. The pH values of the solutions were also measured and significant variations were not found with respect

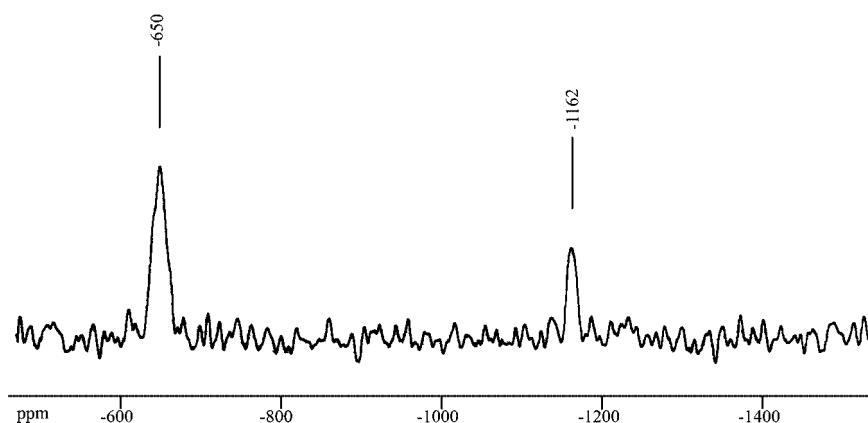
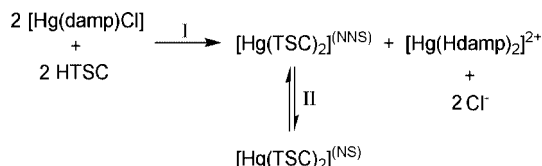


Figure 11. <sup>199</sup>Hg NMR spectrum at room temperature of the reaction between [Hg(damp)Cl] and HA4DM in MeOH/[D<sub>4</sub>]MeOH. The signal for [Hg(Am4DM)<sub>2</sub>] is on the left and that for [Hg(Hdamp)<sub>2</sub>]<sup>2+</sup> on the right.



Scheme 3.

to the typical value for MeOH. This observation is consistent with the presence of the species  $[\text{Hg}(\text{Hdamp})_2]\text{Cl}_2$ , which would retain the protons lost by the ligand upon coordination to mercury.

The reaction between  $[\text{Hg}(\text{damp})\text{Cl}]$  and HAmzp4DH in DMSO was carried out and  $^1\text{H}$  NMR spectra were acquired. It was found that, in addition to the signals corresponding to species **3** (as discussed above), a new set of signals appeared due to the presence of organometallic rings (in the range 7.17–7.48 ppm),  $\text{CH}_2$  ( $\delta$  = 3.47 ppm) and the methyl groups of  $[\text{Hg}(\text{Hdamp})_2]\text{Cl}_2$  ( $\delta$  = 2.23 ppm). Furthermore, the presence of a singlet at  $\delta$  = 10.26 ppm in the reaction between  $[\text{Hg}(\text{damp})\text{Cl}]$  and HAmzp4DH provides further evidence for protonation of the Hdamp nitrogen. Similarly, in the reaction between  $[\text{Hg}(\text{damp})\text{Cl}]$  and HAm4DM in  $\text{CDCl}_3$ , as well as the signals described above, a signal was observed at  $\delta$  = 11.60 ppm and this is probably due to protonation of the species  $[\text{Hg}(\text{Hdamp})_2]^{2+}$ . Protonation of the ligand Hdamp is supported by IR spectra of damp, which show a band corresponding to  $\nu(\text{N-H})$  vibrations at around  $2670\text{ cm}^{-1}$ , a value consistent with those found for other Hdamp complexes,<sup>[20,31,32]</sup> and with the N-H absorption of free tertiary ammonium salts (ca.  $2700\text{ cm}^{-1}$ ).

## Experimental Section

Elemental analyses were performed with a Carlo Erba 1108 micro-analyser. The mass spectra were obtained using the FAB method with a Hewlett-Packard HP5988A mass spectrometer. IR spectra were recorded as KBr disks ( $4000\text{--}400\text{ cm}^{-1}$ ) or polyethylene-sandwiched Nujol mulls ( $500\text{--}100\text{ cm}^{-1}$ ) with a Bruker IFS-66v spectrometer. NMR spectra were obtained with a Bruker AMX 300 and AMX 500 spectrometers; chemical shifts are reported in ppm downfield from  $\text{Me}_4\text{Si}$  or  $\text{Hg}(\text{CH}_3)_2$ . With the exception of  $[\text{Hg}(\text{Am4DH})_2]$ , the  $^{199}\text{Hg}$  NMR spectra of the other mercury complexes could not be registered due to their low solubility.

$[\text{Hg}(\text{damp})\text{Cl}]$  was synthesised according to the reported procedure.<sup>[33]</sup> The thiosemicarbazones were prepared by reduction of pyridine-2-carboxamide and pyrazine-2-carboxamide with sodium and subsequent reaction with the corresponding thiosemicarbazide as described previously.<sup>[6,34,35]</sup>

**Synthesis of  $[\text{Hg}(\text{Am4DH})_2]$  (1):** A mixture of HAm4DH (0.03 g, 0.15 mmol) and  $[\text{Hg}(\text{damp})\text{Cl}]$  (0.06 g, 0.15 mmol) in methanol (25 mL) was heated under reflux for 1 h. The clear pale-yellow solution was left to crystallise and, after several days, colourless crystals suitable for crystal determination were obtained. Yield: 4.86 mg.  $\text{C}_{14}\text{H}_{16}\text{HgN}_{10}\text{S}_2$  (589.06): calcd. C 28.5, H 2.7, N 23.8, S 10.9; found C 28.6, H 2.6, N 23.2, S 10.1. IR:  $\tilde{\nu}_{\text{max}}$  = 3479–3148  $\nu(\text{NH})$ , 1606–1552  $\nu(\text{C}=\text{N}$  and  $\text{C}=\text{C})$ , 1003  $\nu(\text{NN})$ , 795  $\nu(\text{CS})$ , 415  $\nu(\text{Hg-N})$ , 322  $\nu(\text{Hg-S})\text{ cm}^{-1}$ . FAB<sup>+</sup> MS,  $m/z$  (%), assignment:

196.09 (1.47),  $[\text{H}_2\text{Am4DH}]$ .  $^1\text{H}$  NMR ( $[\text{D}_6]\text{DMSO}$ , ppm):  $\delta$  = 8.44 (d, 1 H, 1-H), 7.83 (d, 1 H, 4-H), 7.67 (td, 1 H, 3-H), 7.36 (m, 1 H, 2-H), 6.60 (s, 2 H,  $\text{N}5\text{H}_2$ ), 6.03 (s, 2 H,  $\text{N}4\text{H}_2$ ).

**Synthesis of  $[\text{Hg}(\text{Am4DM})_2]$  (2):** HAm4DM (0.02 g, 0.1 mmol) in methanol was added to a stirred solution of  $[\text{Hg}(\text{damp})\text{Cl}]$  (0.02 g, 0.1 mmol) in methanol (20 mL). The mixture was stirred for several hours and the resulting yellow solution was left to crystallise. A yellow crystalline solid formed after several days and crystals suitable for X-ray diffraction were obtained from the same solvent. Yield: 15.48 mg.  $\text{C}_{18}\text{H}_{24}\text{HgN}_{10}\text{S}_2$  (645.17): calcd. C 33.5, H 3.7, N 21.7, S 9.9; found C 33.4, H 3.8, N 21.7, S 9.1. IR:  $\tilde{\nu}_{\text{max}}$  = 3489–3358  $\nu(\text{NH})$ , 1609–1544  $\nu(\text{C}=\text{N}$  and  $\text{C}=\text{C})$ , 995  $\nu(\text{NN})$ , 797  $\nu(\text{CS})$ , 418  $\nu(\text{Hg-N})$ , 305  $\nu(\text{Hg-S})\text{ cm}^{-1}$ . FAB<sup>+</sup> MS,  $m/z$  (%), assignment: 646.27 (1.70),  $[\text{Hg}(\text{HAmDM})(\text{Am4DM})]$ ; 559.26 (17.0),  $[\text{Hg}(\text{AmDM})(\text{C}_6\text{H}_8\text{N}_4)]$ ; 423.14 (0.73),  $[\text{Hg}(\text{AmDM})]$ ; 224.12 (3.12),  $[\text{H}_2\text{Am4DM}]$ .  $^1\text{H}$  NMR ( $[\text{D}_6]\text{DMSO}$ , ppm):  $\delta$  = 8.44 (d, 1 H, 1-H), 7.74 (d, 1 H, 4-H), 7.63 (td, 1 H, 3-H), 7.37 (m, 1 H, 2-H), 6.60 (s, 2 H,  $\text{N}5\text{H}_2$ ), 3.08 (s, 6 H, 2Me).

**Synthesis of  $[\text{Hg}(\text{Ampz4DH})_2]$  (3):** A mixture of HAmzp4DH (0.02 g, 0.1 mmol) and  $[\text{Hg}(\text{damp})\text{Cl}]$  (0.04 g, 0.1 mmol) in methanol (25 mL) was heated under reflux for 1 h. The resulting yellow-green precipitate was filtered off and dried under vacuum. Yellow crystals suitable for X-ray structural analysis were obtained from the liquors. Yield: 13.29 mg. Elemental analysis:  $\text{C}_{12}\text{H}_{14}\text{HgN}_{12}\text{S}_2$  (591.04): calcd. C 24.4, H 2.4, N 28.4, S 10.8; found C 24.5, H 2.3, N 28.3, S 10.7. IR:  $\tilde{\nu}_{\text{max}}$  = 3500–3146  $\nu(\text{NH})$ , 1608–1553  $\nu(\text{C}=\text{N}$  and  $\text{C}=\text{C})$ , 1017  $\nu(\text{NN})$ , 855  $\nu(\text{CS})$ , 417  $\nu(\text{Hg-N})$ , 326  $\nu(\text{Hg-S})$ . FAB<sup>+</sup> MS,  $m/z$  (%), assignment: 197.09 (1.64),  $[\text{H}_2\text{Ampz4DH}]$ .  $^1\text{H}$  NMR ( $[\text{D}_6]\text{DMSO}$ , ppm):  $\delta$  = 9.58 (s, 1 H, 4-H), 8.67 (s, 1 H, 1-H), 8.56 (d, 1 H, 2-H), 6.61 (s, 2 H,  $\text{N}5\text{H}_2$ ), 6.37, 6.06 (1 H, 1 H, s, s,  $\text{N}4\text{H}_2$ ).

**Synthesis of  $[\text{Hg}(\text{Ampz4DM})_2]$  (4):** HAmzp4DM (0.02 g, 0.09 mmol) in methanol was added to a stirred solution of  $[\text{Hg}(\text{damp})\text{Cl}]$  (0.02 g, 0.09 mmol) in methanol (20 mL). The mixture was stirred for several hours and the resulting yellow solution was left to crystallise. A yellow crystalline formed after several days and was filtered off and dried under vacuum. Yellow crystals suitable for X-ray diffraction were obtained from the same solvent. Yield: 8.74 mg.  $\text{C}_{16}\text{H}_{22}\text{HgN}_{12}\text{S}_2$  (647.14): calcd. C 29.7, H 3.4, N 26.0, S 9.9; found C 29.4, H 3.4, N 25.5, S 10.1. IR:  $\tilde{\nu}_{\text{max}}$  = 3420–3312  $\nu(\text{NH})$ , 1607–1573  $\nu(\text{C}=\text{N}$  and  $\text{C}=\text{C})$ , 1019  $\nu(\text{NN})$ , 861  $\nu(\text{CS})$ , 405  $\nu(\text{Hg-N})$ , 289  $\nu(\text{Hg-S})$ . FAB<sup>+</sup> MS,  $m/z$  (%), assignment: 648.20 (34.03),  $[\text{Hg}(\text{HAmpzDM})(\text{Ampz4DM})]$ ; 423.08 (2.01),  $[\text{Hg}(\text{Ampz4DM})]$ ; 225.10 (5.07),  $[\text{H}_2\text{Ampz4DM}]$ ; 191.12 (55.29),  $(\text{C}_8\text{H}_{11}\text{N}_6\text{S})$ .  $^1\text{H}$  NMR ( $[\text{D}_6]\text{DMSO}$ , ppm):  $\delta$  = 8.84 (s, 1 H, 4-H), 8.58 (s, 1 H, 1-H), 8.48 (s, 1 H, 2-H), 6.51 (s, 2 H,  $\text{N}5\text{H}_2$ ), 3.14 (s, 6 H, 2Me).

**X-ray Crystallography:** Crystals of all complexes were mounted on glass fibres and used for data collection. Crystal data were obtained with a Bruker SMART CCD-1000 diffractometer at room temperature. X-ray data were processed using the SAINT program<sup>[36]</sup> and corrected for absorption using SADABS.<sup>[37]</sup> Structural solution and refinement was carried out using the SHELX suite of programs.<sup>[38,39]</sup> The hydrogen atoms were located unambiguously from difference Fourier maps (N-H hydrogen atoms) and included as fixed contributions riding on attached atoms or included in geometrically idealized positions employing appropriate riding models, all with isotropic displacement parameters constrained to 1.2 times those of their carrier atoms. Atom scattering factors were taken from the International Tables for Crystallography<sup>[40]</sup> and molecular graphics were obtained from PLATON<sup>[41]</sup> (see also Table 6).

Table 6. Crystallographic data for complexes 1–4.

	[Hg(Am4DH) <sub>2</sub> ]	[Hg(Am4DM) <sub>2</sub> ]	[Hg(Ampz4DH) <sub>2</sub> ]	[Hg(Ampz4DM) <sub>2</sub> ]
Empirical formula	C <sub>14</sub> H <sub>16</sub> HgN <sub>10</sub> S <sub>2</sub>	C <sub>18</sub> H <sub>24</sub> HgN <sub>10</sub> S <sub>2</sub>	C <sub>12</sub> H <sub>14</sub> HgN <sub>12</sub> S <sub>2</sub>	C <sub>16</sub> H <sub>22</sub> HgN <sub>12</sub> S <sub>2</sub>
Colour, habit	prism, colourless	yellow, plate	yellow, prism	yellow, prism
Formula weight	589.08	645.18	591.06	647.17
Crystal size [mm]	0.57 × 0.26 × 0.18	0.14 × 0.11 × 0.06	0.16 × 0.14 × 0.11	0.18 × 0.17 × 0.06
Crystal system	monoclinic	orthorhombic	monoclinic	orthorhombic
Space group	C2/c (No. 15)	Pna2 <sub>1</sub> (No. 33)	C2/c (No. 15)	C22 <sub>2</sub> (No. 20)
Unit cell dimensions				
<i>a</i> [Å]	16.907(4)	17.892(3)	13.316(3)	11.898(4)
<i>b</i> [Å]	7.194(2)	9.070(2)	7.805(2)	11.513(4)
<i>c</i> [Å]	15.535(3)	13.915(3)	18.517(4)	16.605(5)
<i>a</i> [°]	90	90	90	90
<i>β</i> [°]	94.781(4)	90	109.648(3)	90
<i>γ</i> [°]	90	90	90	90
<i>V</i> [Å <sup>3</sup> ]	1883.0(7)	2258.2(7)	1812.4(7)	2274.6(13)
<i>Z</i>	4	4	4	4
<i>D</i> <sub>calcd.</sub> (g·cm <sup>−3</sup> )	2.078	1.898	2.166	1.890
<i>μ</i> [mm <sup>−1</sup> ]	8.419	7.029	8.750	6.981
<i>θ</i> Range for data coll. [°]	2.42–26.35	2.28–26.37	2.34–28.28	2.45–28.28
Index ranges	−20 ≤ <i>h</i> ≤ 20 −8 ≤ <i>k</i> ≤ 8 −19 ≤ <i>l</i> ≤ 19	−22 ≤ <i>h</i> ≤ 0 −11 ≤ <i>k</i> ≤ 0 0 ≤ <i>l</i> ≤ 17	−16 ≤ <i>h</i> ≤ 17 0 ≤ <i>k</i> ≤ 10 −24 ≤ <i>l</i> ≤ 0	0 ≤ <i>h</i> ≤ 15 −15 ≤ <i>k</i> ≤ 15 0 ≤ <i>l</i> ≤ 22
Reflections collected	7619	19433	11513	10875
Unique reflects., <i>R</i> <sub>int</sub>	1914, 0.0341	2415, 0.0672	2221, 0.0334	2756, 0.0307
Data/parameters	1914/131	2415/280	2221/123	2756/141
Final <i>R</i> indices	<i>R</i> <sub>1</sub> = 0.0205	<i>R</i> <sub>1</sub> = 0.0430	<i>R</i> <sub>1</sub> = 0.0244	<i>R</i> <sub>1</sub> = 0.0311
[ <i>I</i> > 2σ( <i>I</i> )]	<i>wR</i> <sub>2</sub> = 0.0503	<i>wR</i> <sub>2</sub> = 0.0867	<i>wR</i> <sub>2</sub> = 0.0427	<i>wR</i> <sub>2</sub> = 0.0815
<i>R</i> indices (all data)	<i>R</i> <sub>1</sub> = 0.0220 <i>wR</i> <sub>2</sub> = 0.0510	<i>R</i> <sub>1</sub> = 0.0994 <i>wR</i> <sub>2</sub> = 0.1107	<i>R</i> <sub>1</sub> = 0.0380 <i>wR</i> <sub>2</sub> = 0.0466	<i>R</i> <sub>1</sub> = 0.0379 <i>wR</i> <sub>2</sub> = 0.0878
Goodness-of-fit	1.101	1.097	1.082	1.058
Flack parameter	—	0.09(2)	—	0.00(1)

CCDC-600478 (for [Hg(Am4DH)<sub>2</sub>]), -600479 (for [Hg(Am4DM)<sub>2</sub>]), -600480 (for [Hg(Ampz4DH)<sub>2</sub>]) and -600481 (for [Hg(Ampz4DM)<sub>2</sub>]) contain the supplementary crystallographic data for this paper. These data can be obtained free of charge from The Cambridge Crystallographic Data Centre via [www.ccdc.cam.ac.uk/data\\_request/cif](http://www.ccdc.cam.ac.uk/data_request/cif).

## Acknowledgments

We thank the Xunta de Galicia (Project PGIDIT03PXIC20302PN) for continued financial support.

- [1] D. X. West, S. B. Padhye, P. B. Sonawane, *Struct. Bonding (Berlin)* **1991**, 76, 1–50.
- [2] E. Bermejo, R. Carballo, A. Castiñeiras, R. Domínguez, C. Maichle-Mössmer, J. Strahle, D. X. West, *Polyhedron* **1999**, 18, 3695–3702.
- [3] E. Bermejo, R. Carballo, A. Castiñeiras, R. Domínguez, A. E. Liberta, C. Maichle-Mössmer, M. M. Salberg, D. X. West, *Eur. J. Inorg. Chem.* **1999**, 965–973.
- [4] A. Castiñeiras, I. García, E. Bermejo, K. A. Ketcham, D. X. West, A. K. El-Sawaf, *Z. Anorg. Allg. Chem.* **2002**, 628, 492–504.
- [5] E. Bermejo, A. Castiñeiras, I. García, D. X. West, *Polyhedron* **2003**, 22, 1147–1154.
- [6] I. García Santos, PhD Thesis, University of Santiago de Compostela, Spain, **2001**.
- [7] E. Bermejo, R. Carballo, A. Castiñeiras, R. Domínguez, A. E. Liberta, C. Maichle-Mössmer, D. X. West, *Z. Naturforsch. Teil A* **1999**, 54, 777–787.
- [8] E. Bermejo, A. Castiñeiras, R. Domínguez, R. Carballo, C. Maichle-Mössmer, J. Strahle, D. X. West, *Z. Anorg. Allg. Chem.* **1999**, 625, 961–968.
- [9] R. Carballo, A. Castiñeiras, T. Pérez, *Z. Naturforsch. Teil A* **2001**, 56, 881–888.
- [10] I. García Santos, U. Abram, R. Alberto, E. Vázquez López, A. Sánchez, *Inorg. Chem.* **2004**, 43, 1834–1836.
- [11] I. García Santos, A. Castiñeiras, U. Abram, unpublished results.
- [12] J. L. Wardell, in *Comprehensive Organometallic Chemistry* (Ed.: G. Wilkinson), vol. 2, Pergamon, Oxford, **1982**.
- [13] T. S. Lobana, *Coord. Chem. Rev.* **1985**, 63, 161–215.
- [14] T. S. Lobana, M. K. Sandhu, D. C. Povey, G. W. Smith, *J. Chem. Soc., Dalton Trans.* **1988**, 2913–2914.
- [15] T. S. Lobana, M. K. Sandhu, *Indian J. Chem. Sect. A* **1990**, 29, 394–396.
- [16] T. S. Lobana, A. Sánchez, J. S. Casas, A. Castiñeiras, J. Sordo, M. S. García-Tasende, E. M. Vázquez-López, *J. Chem. Soc., Dalton Trans.* **1997**, 4289–4300.
- [17] T. S. Lobana, A. Sánchez, J. S. Casas, A. Castiñeiras, J. Sordo, M. S. García-Tasende, *Main Group Met. Chem.* **2001**, 24, 61–62.
- [18] J. Zukerman-Schhpector, M. C. Rodríguez-Argüelles, M. I. Suárez, A. Sánchez, J. S. Casas, J. Sordo, *J. Coord. Chem.* **1991**, 24, 177–182.
- [19] T. S. Lobana, A. Sánchez, J. S. Casas, M. S. García-Tasende, J. Sordo, *Inorg. Chim. Acta* **1998**, 267, 169–172.
- [20] I. García Santos, A. Hagenbach, U. Abram, *Dalton Trans.* **2004**, 677–682.
- [21] L. Pauling, *The Nature of the Chemical Bond*, 3<sup>rd</sup> ed., Cornell University Press, New York, **1960**.
- [22] M. Calvin, K. Wilson, *J. Am. Chem. Soc.* **1945**, 67, 2003–2007.
- [23] G. A. Bogdanović, A. Spasojević-de Bire, S. D. Zarić, *Eur. J. Inorg. Chem.* **2002**, 1599–1609.
- [24] a) M. Nishio, M. Hirota, Y. Umezawa, *The CH/π Interactions*, Wiley-VCH, New York, **1998**; b) T. Steiner, *Angew. Chem. Int. Ed.* **2002**, 41, 48–76.



- [25] T. S. Lobana, A. Sánchez, J. S. Casas, A. Castiñeiras, J. Sordo, M. S. García-Tasende, *Polyhedron* **1998**, *17*, 3701–3709.
- [26] J. S. Casas, E. E. Castellano, M. S. García-Tasende, A. Sánchez, J. Sordo, E. M. Vázquez-López, J. Zukerman-Schepector, *J. Chem. Soc., Dalton Trans.* **1996**, 1973–1978.
- [27] L. G. Makarova, A. N. Nesmeyanov, *The Organic Compounds of Mercury*, North-Holland, Amsterdam, **1967**.
- [28] C. A. McAuliffe, *The Chemistry of Mercury*, Macmillan, London, **1977**.
- [29] R. C. Larock, Organomercury Compounds, in *Organic Synthesis*, Springer, Berlin, **1985**.
- [30] W. J. Geary, *Coord. Chem. Rev.* **1971**, *7*, 81–122.
- [31] U. Abram, K. Ortner, R. Gust, K. Sommer, *J. Chem. Soc., Dalton Trans.* **2000**, 735–744.
- [32] J. S. Casas, M. V. Castaño, M. C. Cifuentes, J. C. García-Montagudo, A. Sánchez, J. Sordo, U. Abram, *J. Inorg. Biochem.* **2004**, *98*, 1009–1016.
- [33] J. Mack, K. Ortner, U. Abram, R. V. Parish, *Z. Anorg. Allg. Chem.* **1997**, *268*, 191.
- [34] A. Castiñeiras, I. García, E. Bermejo, D. X. West, *Polyhedron* **2000**, *19*, 1873–1880.
- [35] L. M. Fostiak, I. García, J. K. Swearingen, E. Bermejo, A. Castiñeiras, D. X. West, *Polyhedron* **2003**, *22*, 83–92.
- [36] Bruker, SMART and SAINT. *Area Detector Control Integration Software*, Bruker Analytical X-ray Instruments, Inc., Madison, Wisconsin, USA, **1999**.
- [37] G. M. Sheldrick, SADABS. *Program for Empirical Absorption Correction of Area Detector Data*, University of Göttingen, Germany, **1997**.
- [38] G. M. Sheldrick, *Acta Crystallogr., Sect. A* **1990**, *46*, 467–473.
- [39] G. M. Sheldrick, SHELX-97. *Program for the Refinement of Crystal Structures*, University of Göttingen, Germany, **1997**.
- [40] A. J. C. Wilson, *International Tables for Crystallography*, vol. C, Kluwer Academic Publishers, Dordrecht, The Netherlands, **1995**.
- [41] A. L. Spek, PLATON. *A Multipurpose Crystallographic Tool*, Utrecht University, Utrecht, The Netherlands, **2003**.

Received: March 30, 2006

Published Online: June 6, 2006